EUROPEAN FUSION DEVELOPMENT AGREEMENT
JET

EFDA–JET–CP(04)03-32

Y.Q. Liu, T.C. Hender, M. Gryaznevich, D.F. Howell, S.D. Pinches, R.J. Buttery,
A. Bondeson and JET EFDA Contributors

Modelling of Resistive Wall Mode Experiments in JET

Modelling of Resistive Wall Mode Experiments in JET

Y.Q. Liu[1], T.C. Hender[2], M. Gryaznevich[2], D.F. Howell[2],
S.D. Pinches[3], R.J. Buttery[2], A. Bondeson[1] and JET EFDA contributors*

[1] Department of Electromagnetics, EURATOM/VR Fusion Association, Chalmers University of Technology, Göteborg, Sweden
[2]EURATOM/UKAEA Fusion Association, Culham Science Centre, Abingdon, Oxon, OX14 3DB, UK
[3] Max-Plank Institute for Plasmaphysik, EURATOM-Assoziation, Garching, Germany
** See annex of J. Pamela et al, "Overview of Recent JET Results and Future Perspectives", Fusion Energy 2002 (Proc. 19th IAEA Fusion Energy Conference, Lyon (2002).*

Preprint of Paper to be submitted for publication in Proceedings of the
31st EPS Conference,
(London, UK. 28th June - 2nd July 2004)

INTRODUCTION

Advanced tokamaks have favorable micro-instabilities and thereby good transport prop-erties, but the operational space (in terms of achievable pressure limits) is limited by ideal external kink modes, with low toroidal mode numbers $n = 1, 2, 3$. A conducting wall sup-presses the instability at the resistive decay time of the wall eddy currents. At longer time scale, the stabilization is lost and the resulting slowly growing mode is called Resistive Wall Mode (RWM). The RWM need to be stabilized in order to achieve steady state operation at high plasma pressures for advanced tokamaks. Indeed, for an advanced scenario in ITER, the normalized plasma pressure $\beta_N \equiv \beta(\%)/[I(\mathrm{MA})/a(\mathrm{m})B(\mathrm{T})]$ can be increased from about 2.5 (no-wall beta limit) to about 3.5 (ideal-wall limit), if the RWMis stabilized [1].

Both JET RWM experiments and simula-tions using the stability code MARS-F aim at understanding physics of the RWM. From the modeling point of view, the key issue is the choice of adequate damping models, that are used in the MARS-F code. The correct pre-diction of experimental results depends sen-sitively on the damping models [2]. There-fore, the RWM experiments benchmark different models, that then lead to better under-standing of the RWM physics.

Two types of experiments on JET are modeled. The first is the minimal (critical) plasma toroidal rotation speed needed in order to stabilize the mode. The second is the Resonant Field Amplification (RFA) experiments, which can be viewed as the MHD spectroscopy for the RWM. In this paper, we studied only the $n = 1$ RWM.

1. DAMPING MODELS

At least two types of dissipation play im-portant roles in the stabilization of RWM by plasma rotation. One comes from the Alfvénic resonances (“Afvén continuum damping”) that is described by ideal MHD.

The other dissipation comes from ion Landau damping for the ion motion along the field lines. This kinetic effect is modeled as addi-tional terms in MHD equations in the MARS-F code. We considered a parallel viscosity term

$$\vec{F}_{\mathrm{visc}} = -\kappa_{\|}|k_{\|}|v_{th,i}\,\rho\vec{v}_{\|} \tag{1}$$

which represents the parallel sound wave damping, with a free parameter $\kappa_{\|}$ for the model. We also introduced a more physics-based semi-kinetic damping model where the damping force is computed from the imaginary part of the kinetic energy perturbation, calculated for a cylindrical plasma [3].

2. CRITICAL PLASMA ROTATION

We chose an equilibrium reconstructed from the JET Pulse No: 62024. The toroidal vacuum field is about 1.2T, and the total plasma current is about 1.0MA. The plasma has rather broad current profile, with the internal inductance $l_i = 0.73$. The computed β_N limits are 2.63 without the wall and 3.36 with the ideal JET wall. We computed the critical plasma rotation speed versus a parameter C_β

defined as $C_\beta \equiv (\beta_N - \beta_N^{\text{no-wall}})/(\beta_N^{\text{ideal-wall}} - \beta_N^{\text{no-wall}})$, using different damping models as shown in Fig.1. The sound wave damping model predicts different critical rotation speed depending on the choice of $\kappa_{||}$. Comparison with the experimental data indicates that either strong sound wave damping (i.e. with large coeffi-cient $\kappa_{||}$), or semi-kinetic damping model re-produces the correct values for the critical rotation. Generally there is no strong dependence of critical rotation on the plasma pressure. For the JET plasma, the critical rotation speed at the $q = 2$ surface is about 0.5% of the toroidal Alfvén speed ν_A. We note that the typical plasma rotation speed in JET is much larger (about 1.7% ν_A at $q = 2$ for the shot considered here) than the critical rotation. Therefore, the RWM is usually well damped in JET plasmas.

3. RESONANT FIELD AMPLIFICATION

3.1. GEOMETRY

In JET RFA experiments, the error fields are produced by currents flowing in the inter-nal saddle coils or in the Error Field Correction Coils (EFCC). Figure 2 shows the geometry for the MARS-F modeling of RFA experiments. The JET wall is modeled as a complete thin shell. Both internal saddles and EFCC are modeled as infinite number of coils along the toroidal direction, that produce an exp ($jn\phi$) dependence of the current density along the ϕ angle. The radial and poloidal locations of the saddle and pick-up coils are the same as in the experiments. We also include a thin shell with a poloidal gap in the outboard mid-plane (dashed line in Fig.2), in order to repre-sent the effect of 3D conducting structures lo-cated in JET between the EFCC and the pick-up coils. Without the second shell, it is not possible to reproduce the RFA experiments with EFCC and AC excitation currents.

3.2. RFA WITH INTERNAL SADDLES

First we modeled the RFA experiments where the error field is produced by a DC current in the saddle coils. We compared both the amplitude and the phase of the amplification factor, and found that the code can reproduce the experimental results only if a strong sound wave damping or the semi-kinetic damping is included. In all the RFA simulations in this paper, we chose the semi-kinetic damping model. The RWM in JET is also excited by standing waves launched by the saddle coils. Two flux signals are measured: one is in phase (toroidally) with the saddle coils (MHDF signal in JET), the other is in 90^o toroidal phase shift with the saddles (MHDG). In MARS-F simulations, we launch traveling waves. The plasma responses from two traveling waves, with the same frequency but opposite toroidal directions, are then combined to obtain the response for a standing wave. Traveling waves give more rich information about the plasma response.

Figure 3 shows the comparison of the JET vacuum shots (i.e. with only the saddles and walls but no plasma) and the MARS-F modeling. Plotted are the amplitude (normalized by the value at zero frequency) of the sensor flux (MHDF-signal in this case), and the temporal phase lag of the signal with respect to the excitation current. A good fit to the experimental data is obtained by MARS-F. The similar comparison is made for the RFA experiments (with all the components including the plasma), as shown in Fig.4 for a wide frequency range from 0 to 120Hz. The agreement between MARS-F modeling and the experiments is reasonable for both amplitude and the temporal phase shift.

The plasma response to an AC external field can be described by a frequency dependent transfer function, in a similar way as we have done for the feedback control of the RWM [4]. We define a function

$$P(j\omega) = \frac{\psi(\omega)}{\psi(\omega = 0 | \text{vacuum})}, \tag{2}$$

where $\psi(\omega)$ is the total flux through the pick-up coils and depends on the excitation frequency ω. The plasma response to a traveling wave is completely described by $P(j\omega)$. The plasma response to a standing wave can be easily constructed from $P(j\omega)$.

The transfer functions for the vacuum and the RFA shots with internal saddle coils are computed by MARS-F and represented by 2-pole Padé approximation

$$\begin{aligned} P_{\text{int}}^{\text{vac}}(j\omega) &= \frac{0.77}{j\omega + 1.0} + \frac{0.071}{j\omega + 0.31}, \\ P_{\text{int}}^{\text{RFA}}(j\omega) &= \frac{1.00 + 0.54j}{j\omega + 0.72 - 0.21j} + \frac{-0.029 - 0.017j}{j\omega + 0.22 - 0.48j}, \end{aligned} \tag{3}$$

where ω is normalized by the wall time of the JET wall.

3.3. RFA WITH EFCC

The RFA experiments with EFCC are also modeled by MARS-F. We found that it is easy for MARS-F to recover the plasma response to the static error fields. However, for the time-varying fields, in order to match the data from vacuum shots, we have to introduce a second shell with a poloidal gap, as shown in Fig.2, and adjust the radial position, the poloidal extent of the gap, as well as the wall time for the second shell. The best fit to the experimental data, as shown in Fig.5, corresponds to a thin shell placed at $r = 1.7a$ (a is the plasma minor radius), with poloidal gap covering about 10% of the total poloidal circum-ference, and with the wall time 10 times larger than the JET wall time. It should be noted that once these parameters for the second shell have been fixed in the vacuum matching, the same shell is used consistently in all the other modelings, including those shown in Fig.3, 4, 6. No extra scaling factors have been introduced. Figure 6 shows the comparison of the RFA experimental data with the MARS-F calculations for EFCC. The experimental data are rather scattered due to the variation of the plasma conditions (e.g. the plasma pressure), as well as the fact that the MHDG signal is rather weak compared with MHDF which is dominated by the vacuum field. By the latter reason we show the experimental data only for the MHDG signal. The transfer functions with EFCC are computed as:

$$\begin{aligned} P_{\text{EFCC}}^{\text{vac}}(j\omega) &= \frac{0.37}{j\omega + 1.0} + \frac{0.10}{j\omega + 0.16}, \\ P_{\text{EFCC}}^{\text{RFA}}(j\omega) &= \frac{0.35 + 0.018j}{j\omega + 0.88 - 0.009j} + \frac{0.11 + 0.012j}{j\omega + 0.16 + 0.007j}. \end{aligned}$$

CONCLUSION

Using the MARS-F code, we were able to model the JET RWM experiments, for both the critical plasma rotation required for the RWMstabilization, and the resonant field amplification. The semi-kinetic damping model gives adequate predictions for both critical rotation and RFA. For the RFA experiments in JET, It is important to take into account the influence of the conducting structures between the EFCC and the pick-up coils. We model these structures by a partial wall with a poloidal gap. The plasma responses in the RFA experiments are computed as 2-pole Padé approximations. This study allows RWM stability in ITER to be predicted with better confidence than previously possible.

REFERENCES

[1]. Y.Q. Liu, et al, Nucl. Fusion **44** 232 (2004).

[2]. A. Bondeson, et al, Plasma Phys. Controll. Fusion **45** A253 (2003).

[3]. A. Bondeson and M.S. Chu, Phys. Plasmas **3** 3013 (1996).

[4]. Y.Q. Liu, et al, Phys. Plasmas **7**, 3681 (2000).

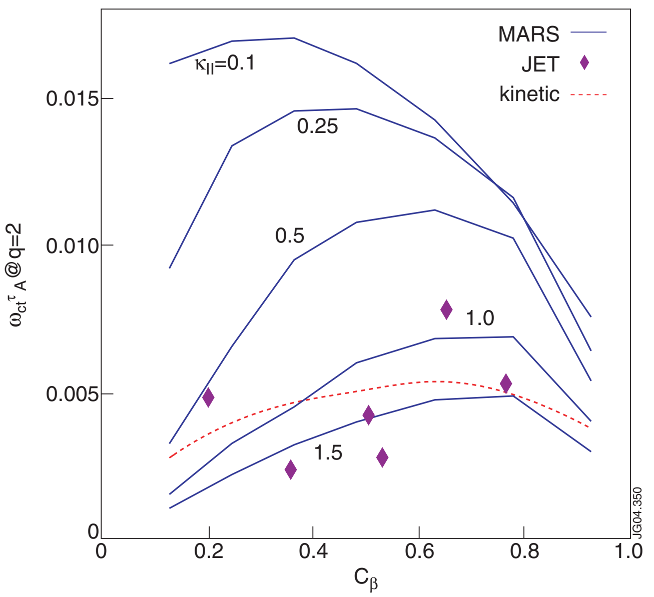

Figure 1: Critical plasma rotation, measured at the q = 2 surface, required to make the RWM marginally stable. MARS-F computations (solid lines) with different damping models are compared with the JET experimental data (filled diamonds).

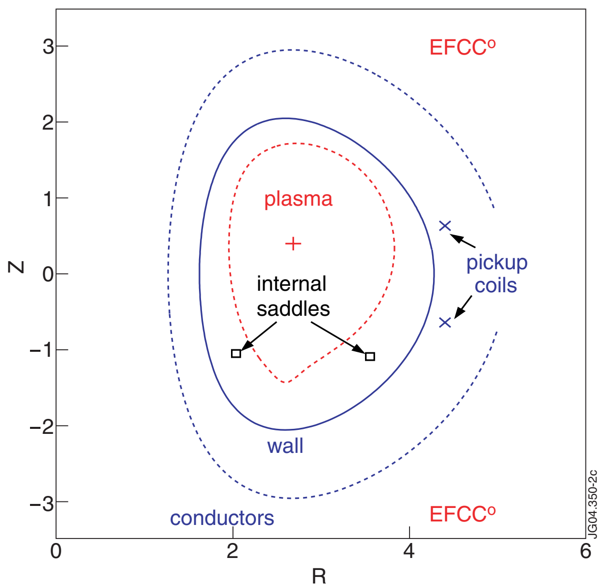

Figure 2: Geometry of RFA experiments on JET with internal saddle coils (squares) and EFCC (circles). The JET 3D conducting structures are modeled as a 2D wall with a poloidal gap (dashed line between the pick-up coils and the EFCC).

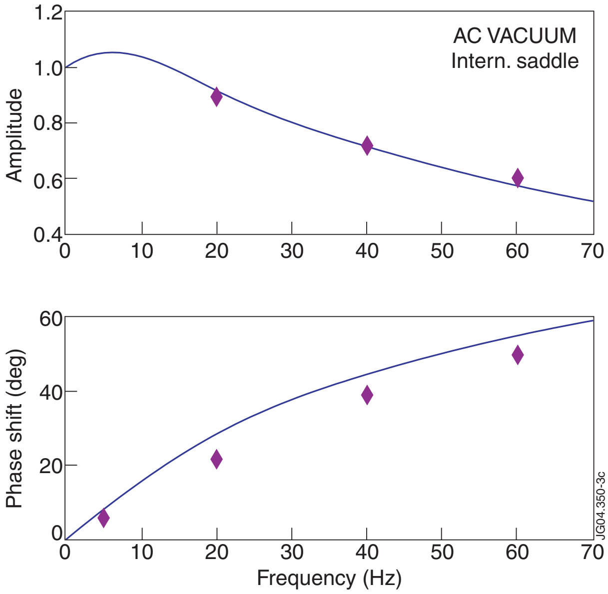

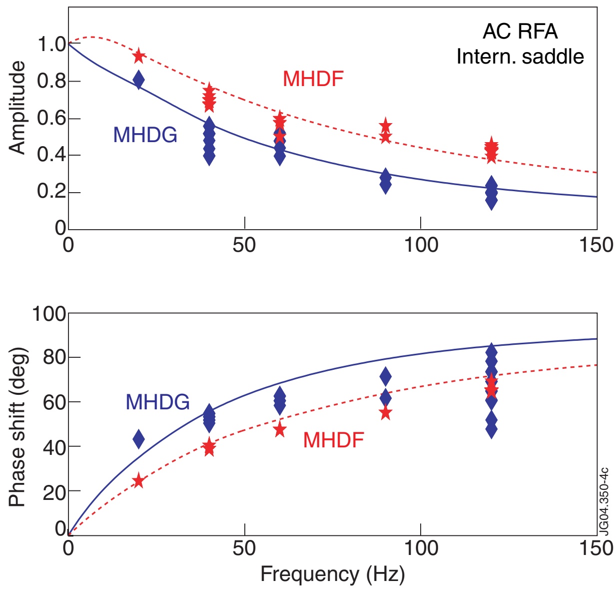

Figure 3: Comparison of JET data (dots) from vacuum shots with MARS-F results (curves) for internal saddle coils with standing waves.

Figure 4: Comparison of JET data (dots) from RFA experiments with MARS-F results (curves) for internal saddle coils with standing waves.

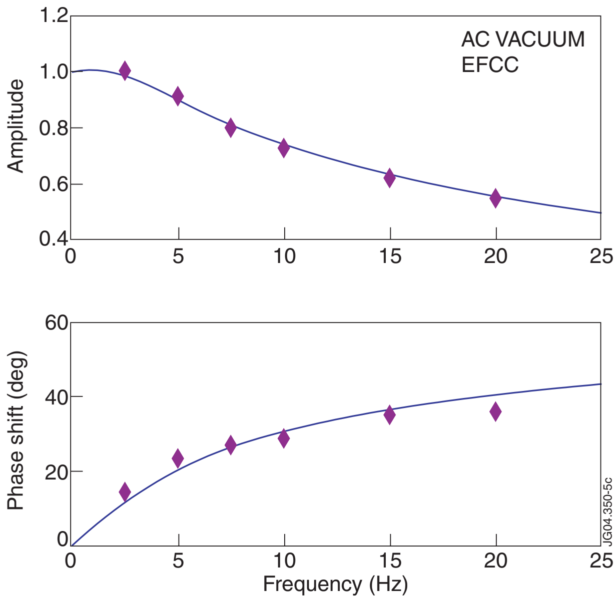

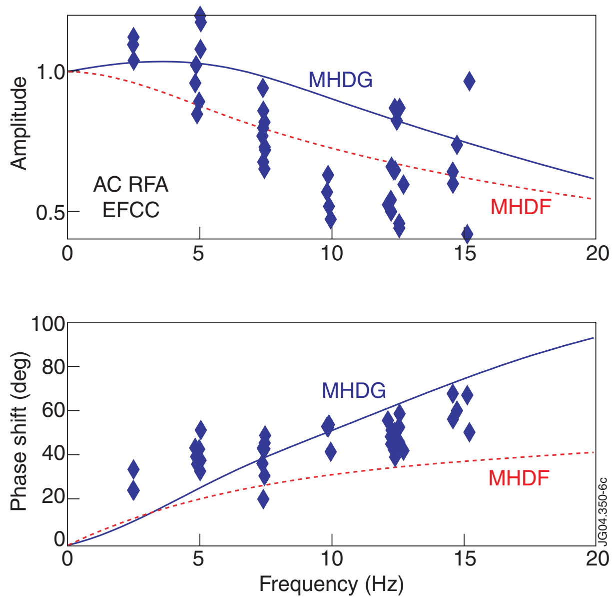

Figure 5: Comparison of JET data (dots) from vacuum shots with MARS-F results (curves) for EFCC with standing waves.

Figure 6: Comparison of JET data (dots) from RFA experiments with MARS-F results (curves) for EFCC with standing waves.